



Ultrasound Vector Flow Imaging: Part II: Parallel Systems

Jensen, Jørgen Arendt; Nikolov, Svetoslav Ivanov; Yu, Alfred C. H.; Garcia, Damien

Published in:

IEEE Transactions on Ultrasonics, Ferroelectrics and Frequency Control

Link to article, DOI:

[10.1109/TUFFC.2016.2598180](https://doi.org/10.1109/TUFFC.2016.2598180)

Publication date:

2016

Document Version

Peer reviewed version

[Link back to DTU Orbit](#)

Citation (APA):

Jensen, J. A., Nikolov, S. I., Yu, A. C. H., & Garcia, D. (2016). Ultrasound Vector Flow Imaging: Part II: Parallel Systems. *IEEE Transactions on Ultrasonics, Ferroelectrics and Frequency Control*, 63(11), 1722 - 1732. <https://doi.org/10.1109/TUFFC.2016.2598180>

General rights

Copyright and moral rights for the publications made accessible in the public portal are retained by the authors and/or other copyright owners and it is a condition of accessing publications that users recognise and abide by the legal requirements associated with these rights.

- Users may download and print one copy of any publication from the public portal for the purpose of private study or research.
- You may not further distribute the material or use it for any profit-making activity or commercial gain
- You may freely distribute the URL identifying the publication in the public portal

If you believe that this document breaches copyright please contact us providing details, and we will remove access to the work immediately and investigate your claim.

Ultrasound Vector Flow Imaging: II: Parallel Systems

Jørgen Arendt Jensen¹, *Fellow, IEEE*, Svetoslav Ivanov Nikolov², Alfred C. H. Yu³ and Damien Garcia⁴

¹Center for Fast Ultrasound Imaging, Department of Electrical Engineering,
Technical University of Denmark, DK-2800 Lyngby, Denmark

²BK Ultrasound, Mileparken, Herlev, Denmark

³Department of Electrical and Computer Engineering, University of Waterloo, Waterloo, ON, Canada

⁴Research Unit of Biomechanics & Imaging in Cardiology,
University of Montreal Hospital, Quebec, Canada

Abstract—The paper gives a review of the current state-of-the-art in ultrasound parallel acquisition systems for flow imaging using spherical and plane waves emissions. The imaging methods are explained along with the advantages of using these very fast and sensitive velocity estimators. These experimental systems are capable of acquiring thousands of images per second for fast moving flow as well as yielding estimates of low velocity flow. These emerging techniques allow vector flow systems to assess highly complex flow with transitory vortices and moving tissue, and they can also be used in functional ultrasound imaging for studying brain function in animals. The paper explains the underlying acquisition and estimation methods for fast 2-D and 3-D velocity imaging and gives a number of examples. Future challenges and the potentials of parallel acquisition systems for flow imaging are also discussed.

I. INTRODUCTION

The paper gives a review of the current development of parallel acquisition systems for flow imaging. Currently, most scanners use a sequential acquisition of data, where a single direction in the image is acquired at a time. For flow estimation, this entails emitting sound in the same direction a number of times and then estimating the velocity from the data as described in the accompanying paper [1] for vector flow or for more traditional systems as described in [2], [3]. This acquisition method severely limits the amount of data available for the estimation and thereby the ability to detect velocity with a high precision as the estimation variance is proportional to the number of observations. Also the dynamic range of the flow is limited as the highest velocity possible to estimate is limited by the pulsing rate, and the lowest velocity is limited by the pulse repetition frequency f_{prf} divided by the number of emissions.

The approach to break these limits is to insonify a large region using either spherical or plane waves, and make a sequence which is repeated over a short time duration. Such acquisition schemes have attracted a lot of attention in the last two decades, and the major principles are described in this review. In Section II methods based on spherical emissions are described, and plane wave emissions are given in Section III for 2-D velocity estimates. Estimation of the full 3-D velocity vector is detailed in Section V.

There are major advantages to such schemes. Foremost they break the tie between frame rate, region of interest (ROI), and precision of the estimates. Continuously available data allow very high frame rates for a large ROI for following the dynamics of e.g. the heart and complex vortices at hundred to thousands of frames per second. Further, the data to average in the estimators are only limited by the stationarity of the flow. This is determined by the flow acceleration and often 128 rather than 8 emissions can be used for velocity estimation, which significantly lowers the velocity variance to give quantitative results. This also makes it easier to derive precise quantitative measures for e.g. volume flow, stenosis degree, turbulence indices, and pressure gradients. For low velocity flow the change is even more pronounced, as the acceleration often is low and both accuracy and detectability can be enhanced by averaging over many emissions. The complete data sets also makes it possible to beamform in any direction. The flow can therefore be precisely tracked in any direction, which makes it possible to employ all the different techniques developed for 2-D and 3-D velocity estimation as described in the accompanying paper [1]. These advantages are shown in the clinical examples attained so far and are described in Section VI.

One drawback of parallel imaging is the huge amount of data and the corresponding calculation demand. Often 20-100 Gbytes of data are acquired from the transducer elements, and full images have to be generated for each emission in 2-D, 3-D, or even 4-D (directional beamforming in a 3-D volume). This is a major challenge, but the evolution in graphics processing units (GPUs) will probably solve this within the next 5-10 years. Also, major efforts are conducted in deriving more efficient beamforming in the Fourier domain, using dual-stage beamforming, row-column probes, or recursive imaging. Many more approach will likely be developed in the following years and the future challenges and possibilities in this exciting field are described in the concluding part of the paper in Section VII.

II. SYNTHETIC APERTURE FLOW IMAGING

Synthetic aperture imaging (SAI), as illustrated in Fig. 1, insonifies a whole region of interest using spherical waves

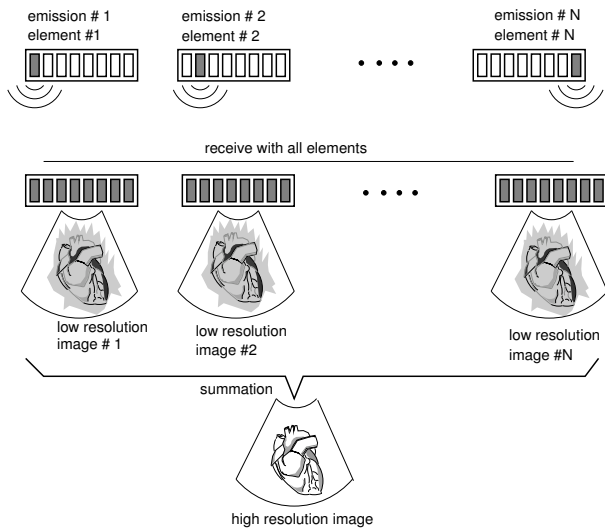


Fig. 1. Acquisition and processing for synthetic transmit aperture imaging. Spherical waves are emitted and the signals received on all transducer elements to yield low resolution images. Combination of these yields a high resolution image dynamically focused in both transmit and receive (from [4]).

[5], [6]. A single element is used in transmit and sends out a spherical wave. Signals are then received on all elements and a full image can be focused in receive to yield a Low Resolution Image (LRI), as there is no transmit focusing. A new element then transmits and yields a new LRI. Combining all the LRIs for all emissions then gives a High Resolution Image (HRI), which is dynamically focused in transmit. This is due to the partial focusing performed in each LRI, where the propagation time from the origin of the emission to the focusing point is taken into account for all points. This results in a dynamic transmit focusing, when all the LRIs are combined.

Focusing is attained by summing the received signals in phase. The geometric distance from the emitting element to the imaging point denoted by \vec{r}_p and back to the receiving element divided by the speed of sound c gives the time instance $t_p(i, j)$ for receiving the sample from the point. This time is [6]:

$$t_p(i, j) = \frac{|\vec{r}_p - \vec{r}_e(i)| + |\vec{r}_p - \vec{r}_r(j)|}{c} \quad (1)$$

where $\vec{r}_e(i)$ denotes the position of the transmitting element i and $\vec{r}_r(j)$ the receiving element j 's position. All points in the LRI are then focused, and this is performed for all LRIs to form the HRI signal $y_f(\vec{r}_p)$:

$$y_f(\vec{r}_p) = \sum_{j=1}^M \sum_{i=1}^N a(t_p(i, j), i, j) y_r(t_p(i, j), i, j) \quad (2)$$

where $y_r(t, i, j)$ is the received signal for emission i on element j , $a(t_p(i, j), i, j)$ is the weighting function (apodization) applied onto this signal, N is the number of transducer elements, and M is the number of emissions. The calculation of both transmit and receive times are dynamic and changed throughout the image. SAI, thus, gives the best possible focusing, when delay-and-sum beamforming is employed and has been extensively studied in the literature [6]. Note that the point \vec{r}_p can be freely selected within the image plane, and focusing can, thus, be attained in any direction and in any order in

the imaging plane. This gives a large flexibility in combining focusing schemes with velocity estimation methods.

SAI has been investigated since the late 1960s and early 1970s [7], [8]. For single element transducers, monostatic SAI has been studied by Ylitalo and Ermert [9]. SAI with arrays has been investigated since the early eighties [10], [11], [12], [8], [13].

In the nineties a method intended for intravascular imaging based on SAI was suggested using a circular aperture [14], [15], [16]. Lockwood and colleagues investigated sparse synthetic aperture systems for 3D imaging applications [17], [18], and Nikolov and Jensen suggested recursive ultrasound imaging [19].

A major problem is the low energy transmitted from a single element and a diverging beam. This was addressed by combining a number of elements to transmit a spherical wave as suggested Karaman et al. [15]. Further combining with coded excitation as suggested by [20], [21], [22], [23], [24] can yield SA ultrasound images with a nearly 50% higher penetration depth than traditional images from the summation of all the LRIs [25]. This has also been demonstrated to yield better clinical images than traditional sequential acquisitions [26], [27], which has led to the introduction of commercial SA scanners. Chiao and colleagues introduced the definition of synthetic transmit aperture (STA) imaging and developed spatial encoding to enable transmission on several elements simultaneously. They separated out the individual transmissions during receive processing using addition and subtraction of the received signals [28]. Another approach by Chiao and Thomas used orthogonal Golay codes to increase the signal-to-noise ratio (SNR) by transmitting simultaneously on several elements [29]. Gran and Jensen suggested to use a division into frequency bands to increase frame rate in SA imaging [30]. This could increase SNR and could be used for velocity estimation [31]. Later a method based on correlation codes was suggested [32].

The major challenge with synthetic aperture flow imaging is that blood scatterers move between emissions and this decorrelates the LRIs. It is illustrated in Fig. 2, where a two-emission SA sequence is shown. The top shows the emission sequence with the point spread function (PSF) for LRIs, and the combined HRIs $H^{(n)}$ are shown at the bottom. The motion is purely axial towards the transducer, and it can be seen that $H^{(n-3)}$ is not directly comparable to $H^{(n-2)}$ due to the different PSFs. However, $H^{(n-1)}$ is a translated version of $H^{(n-3)}$, which has been moved a distance of $2\Delta z = 2v_z T_{prf}$, where v_z is the axial velocity component and T_{prf} is the time between emissions. The LRI PSFs are not perfectly aligned, so the image will be slightly un-sharp but highly correlated between $H^{(n-1)}$ and $H^{(n-3)}$. Ideally the velocity can, thus, be found from any of the methods mentioned in [1]. This was noticed and introduced by Nikolov and Jensen [4], [5], [33].

This might seem like a small detail, but it has major implications for flow estimation. SA imaging insonifies the whole region of interest, so that data are available continuously for all positions. This also makes it possible to beamform in all directions at all places in the image. SA flow sequences can be made short, thus, enabling very fast imaging with hundred

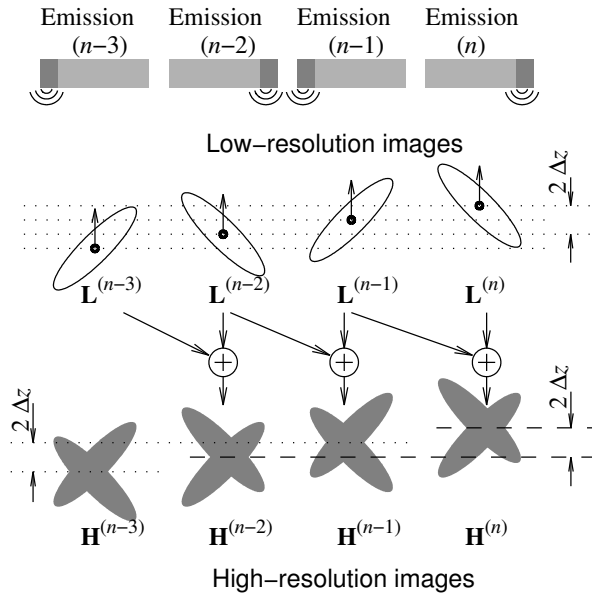


Fig. 2. SA flow imaging uses a short emission sequence. The low resolution point spread functions are combined to yield high resolution images, which pair-wise can be correlated, when the same emission sequence is used. This yields continuous data for the whole image region (from [33]).

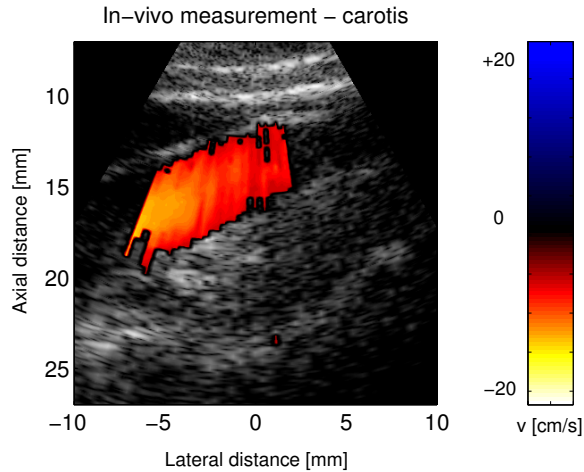


Fig. 3. The first *in-vivo* SA flow imaging obtained. The carotid artery was scanned using only 24 emissions, with the possibility of yielding thousands of images per second (from [33]).

to thousands of frames per second. The continuously available data allow averaging over very long times only limited by the acceleration of the flow to lower the standard deviation of the estimates. It also makes stationary echo canceling easier, as there is no initialization of the filter, so long filter of arbitrary order or complexity can be used.

The fast imaging advantages can be seen from the first *in-vivo* SA flow image shown in Fig. 3, where a four emission long SA sequence was used and repeated six times for a combined total of 24 emissions [33]. This yields 290 frames per second for a pulse repetition frequency f_{prf} of 7 kHz, where a normal frame rate is between 20 to 50 Hz. The f_{prf} could be increased to 25 kHz for this depth resulting

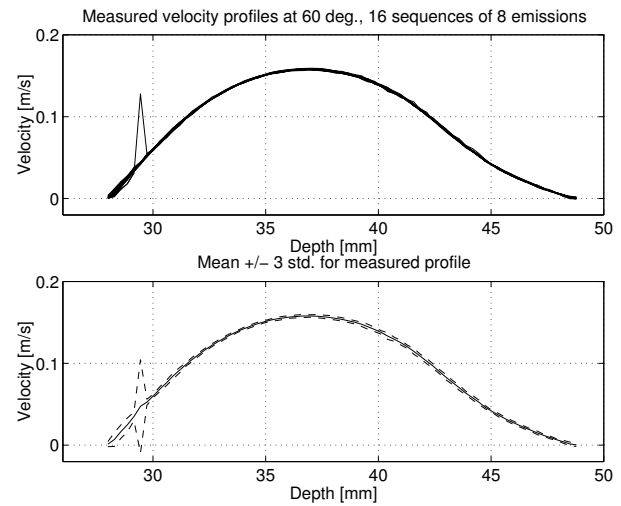


Fig. 4. Flow profiles using directional SA flow imaging. The top graph shows the individual profiles and the bottom graph shows the mean ± 3 standard deviations. The relative SD is 0.3%, thus, yielding fully quantitative flow (from [34]).

in 10,700 images per second, or the whole heart could be covered for a penetration depth of 11 cm. The images can actually be updated at the rate of the pulse repetition frequency as described for recursive SA ultrasound imaging [19]. Here the oldest emission is replaced by the newest one, and an exponential decay can be introduced to gradually decrease the importance of old emissions. This could be adapted to the acceleration of the flow to always have the maximum amount of data for the estimation.

A. Directional beamforming

The advantage of a complete data set has been used in the flow profiles estimated and shown in Fig. 4, where an eight emission long SA sequence was used together with directional beamforming for 128 emissions [34]. The mean profile \pm three standard deviations (SD) are shown in the lower graph, and a relative SD of 0.3% was obtained, which is at least 10 times more accurate than for sequential acquisition systems. In Fig. 4 the angle was known before beamforming or could be estimated from the anatomic image. In the clinic the angle has to be determined for all positions in the image for each frame, and a method to make this was suggested by Jensen and Oddershede [35]. Directional beamforming is here performed in all directions and the normalized correlation function with the highest value indicates the flow angle. Another approach for robust angle estimation was devised by Villagomez-Hoyos et al [36] based on the individual LRIs and then finding the most probable angle.

The inter emission motion will de-correlate the beamformed data, and this degradation has been quantified in [37]. This can for certain combinations of velocities and f_{prf} give a reduction of up to 10 dB for axial motions and 5 dB for lateral motions depending on the set-up. Motion compensation can, however, be applied on the complete data sets to recover some of the loss. This has also been performed for anatomic SA image, where the 2-D motion is estimated from a short SA sequence and used for compensating a long *in-vivo* anatomic SA sequence

[38]. Gran and Jensen suggested to use a frequency division approach for obtaining information from several emissions simultaneously by using separation in the frequency domain [30]. This was combined with the directional beamforming approach to yield velocity estimates [31].

B. Speckle tracking and echo canceling

Speckle tracking can also be used with diverging waves. In 2014 Takahashi et al. showed the feasibility of transthoracic intraventricular vector flow imaging in adults by means of diverging waves emitted by a phased-array [39]. In these *in-vivo* studies, the main challenge was to remove the echo signals generating by the surrounding tissues.

The presence of high-amplitude tissue clutters represents the most major issue of ultrasound cardiac flow imaging, especially when large (instead of focused) wavefronts are transmitted. Clutter filtering has long been the subject of a number of investigations in focused ultrasound imaging [40], [41]. More investigations have to be made to further improve clutter filtering for parallel-beamforming-based imaging. Although more computationally expensive, eigen-based filters may represent a promising approach [42], [43].

C. High dynamic range flow imaging

The fast data frames and continuous data permits detection of both high velocity flow in e.g. the carotid artery [44] and low velocity flow as indicated by Tanter et al [45] for plane wave emissions. A high f_{prf} and cross-correlation approaches or speckle tracking can find the high velocities. The continuous data makes it possible to average over long times only limited by the de-correlation of the correlation functions from the flow acceleration. A high dynamic range can be attained as the data are continuously available at all positions in the image, and this has been used by Villagomez-Hoyos et al [46], [47] to adapt the vector velocity estimation to both high and low velocities. The approach enables the visualization of the flow in both the systolic and diastolic part of the cardiac cycle for the carotid artery, and this could be applied to many other flow situations. The continuous data also makes it possible to have as many spectral displays as needed in the image to visualize the spectral evolution at multiple sites [45].

D. Synthetic aperture sequential beamforming

A major problem in SA imaging and especially in flow imaging is the large amount of calculations. Evolution in GPU processing will solve part of the problem [48], [49], but less demanding schemes for beamforming can also contribute significantly. Kortbek et al. suggested using a dual stage approach called synthetic aperture sequential beamforming (SASB) [50]. This is essentially a mono-static approach where a simple fixed-focused beamformer combines the data and reduces it down to one signal. A second stage dynamic beamformer then makes the high resolution images from a combination of first stage signals. This reduces the data amount and processing demand by a factor of 64, and it was shown to have the same image quality in clinical studies as normal sequential imaging for both linear [51] and non-linear imaging [52].

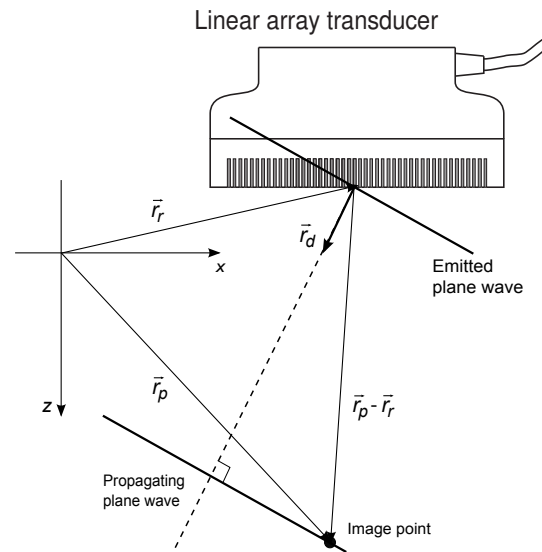


Fig. 5. Plane wave focusing. The geometric distance for the samples to sum are found by the projecting the vector to the image point into the propagation direction of the plane wave.

The approach has been extended by Li and Jensen [53] using SASB and directional beamforming. A full color map image was acquired in 48 emissions using a 4 emission long sequence and had a standard deviation of 4.3% at 65°. Hemmsen et al. has demonstrated that a normal axial cross-correlation estimator and its beamforming can be implemented on a HTC Nexus 9 tablet, where all processing is performed by the Tablet's GPU [54]. This indicates that a fully portable system can be implemented using SA imaging.

III. PLANE WAVE FLOW IMAGING

In plane wave imaging a large region is insonified by emitting a plane wave in a given direction. Usually the full aperture is used and delays are adjusted to yield a wave, which propagates in one direction as shown in Fig. 5. A full low resolution image (no transmit focusing) can then be reconstructed from the received data. The plane wave can be steered in other directions, and multiple emissions can be combined to enhance image quality.

This kind of emissions necessitates a modified delay calculation for the emitted field as illustrated Fig. 5. Here \vec{r}_r is the reference point for the plane wave and \vec{r}_d is a unit vector characterizing its propagation direction. The field point is given by \vec{r}_p and the time t_{dp} it takes the plane wave to arrive at the field point is given by

$$t_{dp} = \frac{\vec{r}_d \cdot (\vec{r}_p - \vec{r}_r)}{c}$$

assuming that emission takes place at time $t = 0$ at \vec{r}_r . The time t_r for the scattered signal to arrive at the receiving element is:

$$t_r(\vec{r}_i, \vec{r}_p) = \frac{|\vec{r}_i - \vec{r}_p|}{c}, \quad (3)$$

which is the geometric distance from the image point to the transducer element position \vec{r}_i divided by the speed of sound c . This assumes that the scattering is spherical and that the speed of sound can be considered constant. The total time from

transmission to reception is then $t_{dp} + t_r(\vec{r}_i, \vec{r}_p)$, which is the time for selecting a sample in the received signal. Multiplied with the sampling frequency gives the sample index for the signals to be summed in the focusing process.

The first to use plane wave imaging for motion estimation was Tanter et al. in 2001 [55], [56], where a single plane wave in transmission was used for transient elastography. The receiving aperture was then split in two for estimating the motion at two different angles similar to multi-beam flow estimation. This gave the motion vector with the advantage of continuously available data for beamforming and estimation. The variance of especially the lateral component could be improved by using tilted plane waves for a number of directions. The motion was then estimated for each of these directions and the resulting motions were averaged to decrease variance. The compounding of estimates were, thus, performed after estimation of the motions.

A. Plane wave speckle tracking

High-frame-rate flow speckle tracking by cross-correlation was first described by Sandrin et al. in 2001 in an experimental vortex [57]. The first *in-vivo* experiments of high frame-rate blood vector velocity imaging was reported in 2005 by Udesen et al. [58], [59]. They used a single plane wave for emission and speckle tracking for flow estimation. Forty speckle images were averaged giving a true frame rate of ~ 100 Hz to yield images with a high temporal and spatial resolution. Time-resolved velocity fields were determined in the frontal plane of the common carotid artery using plane waves. The blood signals were enhanced by temporal high-pass filtering (clutter filtering).

More recently, high-frame-rate speckle tracking was successfully applied in the fast-beating hearts of neonates [60]: in 2014, Fadnes et al. quantified the vector flow in ventricular septal defects transthoracically with a linear array and plane wave transmits.

B. Increasing sensitivity by combining plane waves

Combining more plane waves in the focusing as the approach used in SA imaging in Section II was suggested by Bercoff et al. [45], [48]. Here plane waves are emitted in several directions and low resolution images are focused and combined to a high resolution image for flow estimation. This was used for conventional axial velocity estimation and showed to increase the sensitivity of the estimation at the same time as the advantage of a continuous data stream is available in all parts of the image. The authors call it compounding as presented by [61], where the envelope data is combined or estimates are combined as in [55], [56], but it is important to emphasize that beamformed RF data are combined as in [33]. The number of plane wave directions employed N_p lowers the pulse repetition frequency by a factor of N_p and hence the maximum detectable velocity with the same factor, if a phase or frequency estimator is used. These approaches are, thus, best suited for low velocity flow and this was elegantly demonstrated in scans of a rat brain by Mace et al. [62], [63]. The excellent sensitivity of combined plane wave sequences

was demonstrated in following the evolution of flow in a rat brain (see also Section VI on clinical examples).

C. Multi-direction velocity estimation

In recent years, with a series of advances in research purpose ultrasound imaging systems [64], [65], [66], [67] and channel-domain data acquisition technology [68], [69], [70], new implementations of cross-beam Doppler flow vector estimation have been reported. These newer schemes have appeared in the forms of: (i) single-line, multi-gate flow vector estimation [71], [72], and (ii) flow vector mapping over the entire field of view [73], [74], [75]. One key feature that is shared among these new formulations is the use of plane wave excitation schemes for transmission [76], [77], so as to enhance the frame rate as described earlier in this article. It is worth noting that high-frame-rate, least-squares flow vector estimation technology [78] will become clinically available as a real-time, high-frame-rate diagnostic mode as part of Mindray's new Resona 7 platform in 2016.

Synthetic aperture imaging has also been combined with a spread spectrum approach to increase frame rate by emitted frequency coded waveforms in parallel from a number of elements at the same time [32]. This has also been shown to work for velocity imaging [79].

D. Plane wave transverse oscillation

Plane wave imaging has also been used together with transverse oscillation (TO) to find the 2-D velocity vector for tissue motion [80] and it has also been adapted to blood velocity estimation [81]. An efficient frequency domain estimator was used to find the velocity estimates.

IV. MULTI-LINE TRANSMISSION SCHEMES

An alternative for high-frame-rate blood speckle tracking would be the MLT (multi-line transmit) scheme [82], [83], [84]. In the MLT approach, series of several beams are transmitted at the same time. MLT has not yet been tested in the context of vector flow imaging; whether the MLT cross-talks significantly alter the blood flow signal must be investigated. One way of separating out the parallel beams is to make a frequency division as suggested in [85]. Here the available frequency band is divided into smaller bands suitable for velocity estimation, and this can increase the frame rate by the number of bands or several spectral displays can be made simultaneously.

V. 3-D VECTOR FLOW IMAGING

3-D vector flow imaging has been developed for a single plane using the TO approach by Holbek [86]. Here a 32×32 Vermon matrix array was used and focused emissions in five directions were continuously made to attain frame rates up to 2.1 kHz. An example from the carotid artery is shown in Fig. 6 for two different time points in the cardiac cycle. The example demonstrated the possibility of finding the full 3-D vector with a good precision at a very high frame rate. The approach has now been extended to row-column probes [87],

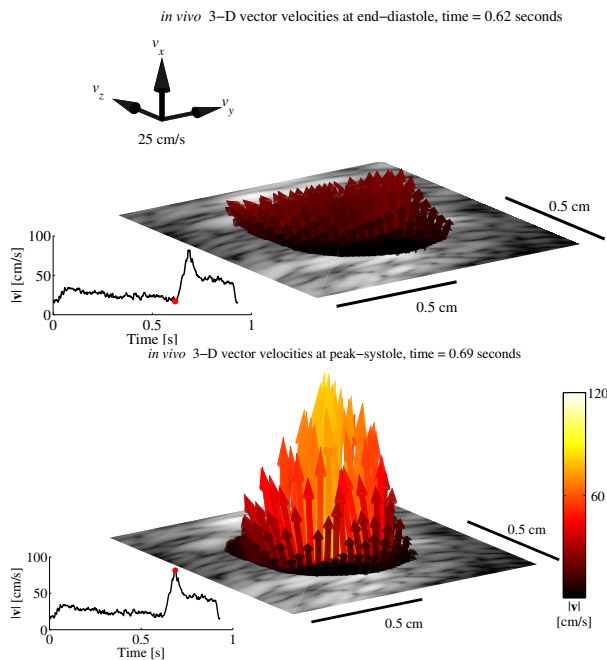


Fig. 6. 3-D vector flow images from the carotid artery using the 3-D TO approach. The arrows indicate velocity magnitude and directions at the diastolic (top) and peak systolic phase (bottom) of the cardiac cycle. The peak velocity magnitude in systole is 0.82 m/s and 0.17 m/s in diastole (from [86]).

which uses 64 + 64 elements rather than the 1024 elements in the fully populated matrix array. A plane wave is emitted in two orthogonal planes, and the velocity full velocity vector is estimated.

Directional beamforming for 3-D SA imaging has also been simulated in [88], which showed that beamformation can be done in all directions and the flow found, if a suitable matrix probe is available. The simulations showed the possibility of acquiring 60 volumes per second with a standard deviation of 3.27% on the velocity estimates.

Provost et al. demonstrated a method for acquiring full 3-D volume data using spherical and plane wave emissions and a 32 × 32 Vermon matrix array [89]. The velocity could be detected *in-vivo* in the heart for 2,325 volumes per second using a power Doppler approach.

VI. CLINICAL APPLICATIONS

The number of clinical studies for parallel flow systems is still limited due to the complicated data acquisition and processing. Experimental ultrasound systems have to be used [64], [65], [67] and often Gigabytes of data must be stored and processed off-line for several days before the results are available.

A. Validation of SA flow imaging

The first example of *in-vivo* SA flow imaging was given by Nikolov and Jensen [33] as shown in Fig. 3. The first validation of SA flow was conducted by Hansen et al. [44] where three vector flow methods were compared including SA directional flow imaging. Eight emissions were used for the flow sequences and phased contrast MRI was used as

a reference when scanning the carotid artery. The stroke volume estimated by the methods were compared for 11 volunteers. Echo canceling was a challenge, but using a dual filter approach a correlation value R of 0.95 between SA and MRI stroke volume was found with a mean difference of 0.07 ml for a range of stroke values from 3.0 and 10.8 ml.

B. Plane wave speckle tracking

The first clinical examples of vector flow imaging using plane waves and speckle tracking were shown by Udesen et al. [58], [59] for the carotid artery, and later a number of different images and video sequences were shown by Hansen et al. [90]. An example from the jugular vein and the carotid artery is shown in Fig. 7. An incompetent valve is shown in the jugular vein for three different time points in the cardiac cycle. The first image on the left shows the flow going from right to left and the vortex behind the valve leaflet is in the clockwise direction. The second image shows reversed flow and that the vortex is in the anti-clockwise direction. The right most image shows secondary rotational flow in the carotid artery on the bottom, and this underlies the complex 3-D velocity in the human circulation. The images are an illustration of the ability of the fast parallel systems to reveal this complex flow with both a high spatial and temporal resolution with hundreds or even thousands of frames per second, which no other image modality currently is capable of.

Echo-PIV has also been combined with plane wave imaging. A technical limitation of echo-PIV is, mostly in the cardiac context, the restricted frame rate obtainable with the conventional scanners. Line-by-line sequential scans limit cardiac B-mode imaging at roughly 50-80 frames/s. To get optimal conditions (200 frames/s), the width and depth of the scan area must be reduced [92]. Intracardiac echo-PIV with conventional ultrasound scanners is therefore not accessible to children or to patients with tachycardia or under cardiac stress triggered by exercise or dobutamine (stress echocardiography). Parallel beamforming in reception can speed up the frame rates of cardiac images up to 5-10 times [82], [93], [94], which can thus solve the frame rate dilemma.

C. Quantification of congenital septal defects

A ventricular septal defect is a congenital heart disease in which there is an opening in the interventricular septum, the wall that separates the two ventricles. During heart contraction, a part of the oxygen-rich blood goes back to the pulmonary circulation, making the heart and lungs work harder. Significant ventricular septal defects need surgical repair early in life to prevent cardiac and pulmonary complications. Echocardiography plays a key role in the diagnosis and planning for the therapeutic approach. Fadnes et al. and Angelelli et al. proposed an innovative tool for better visualization and quantification of septal defects in neonates [95], [60]. They used a linear array emitting plane waves, and applied high-frame-rate ultrasound speckle tracking (without contrast agent) to determine the peak velocities in the opening as shown in Fig. 8. Like in carotid artery stenoses, 2-D vector flow imaging avoided the angle and Doppler gate position issues. Using a

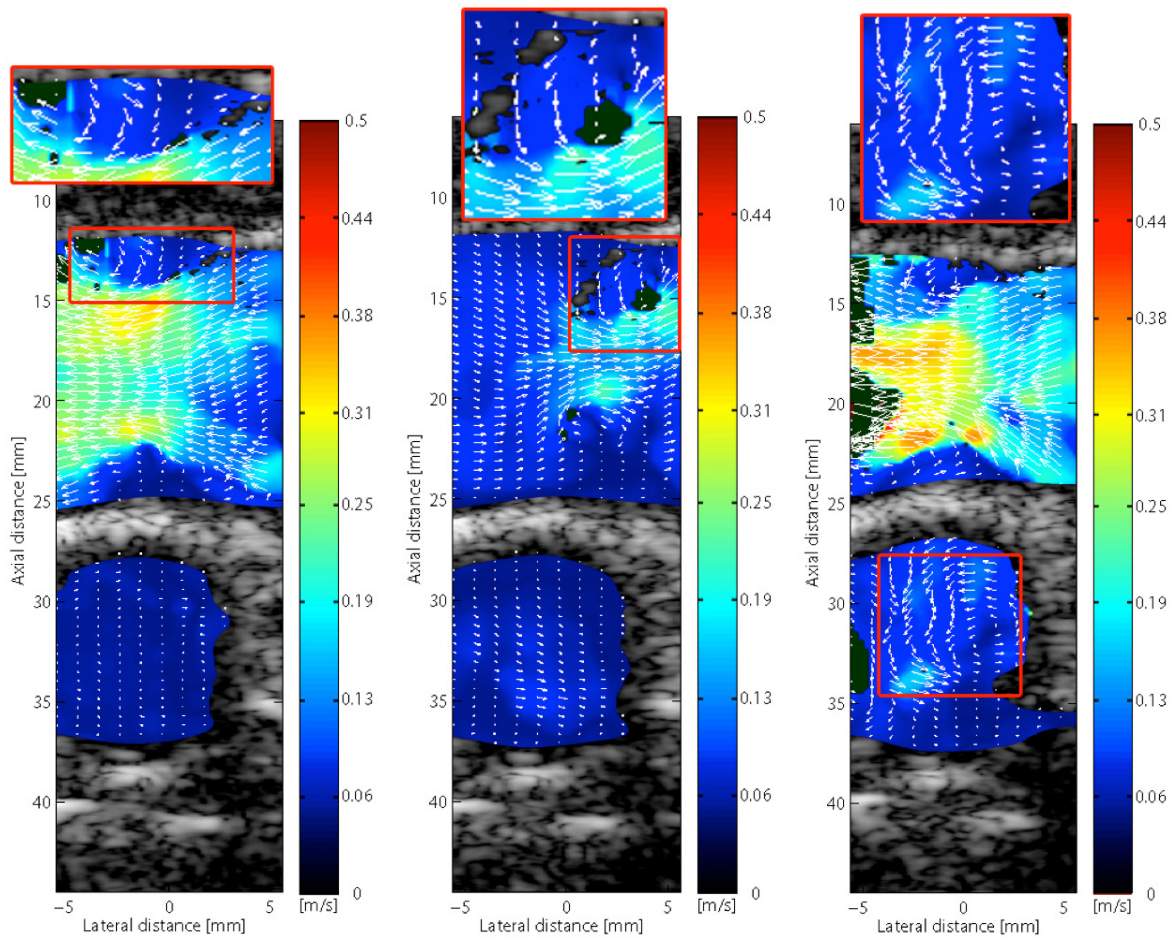


Fig. 7. Plane wave vector flow imaging of the jugular vein (top vessel) and the carotid artery for three different times in the cardiac cycle (from [91]). Note the clock-wise vortex in the left image, and the counter clock-wise vortex behind the incompetent valve leaflet in the middle image.

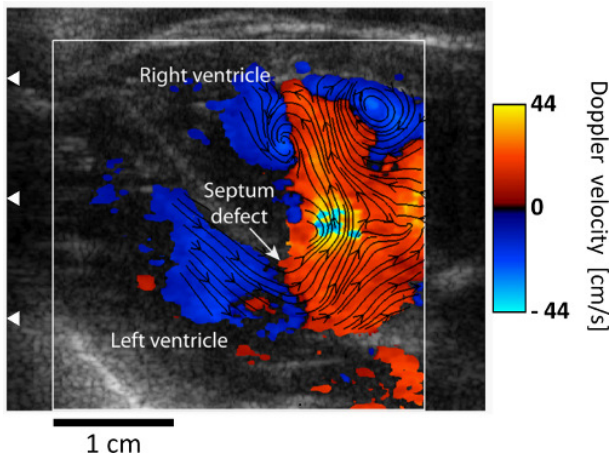


Fig. 8. High-frame-rate vector flow imaging in a neonate ventricular septal defect using high-frame-rate speckle tracking [60]. The streamlines are superimposed on axial velocity estimates for better visualization.

particle-based flow visualization technique, they also generated cine loops, which highlighted the shunt flow very clearly as shown in Fig. 8.

D. Low velocity flow estimation

The ability of plane wave flow imaging to estimate and show low velocity flow was demonstrated by [62], [63] as shown in Fig. 9, which compares a normal flow image (left) to a plane wave power Doppler image (middle). It shows how the continuous data can be used to increase sensitivity and detectability for flow imaging. The last image shows a functional ultrasound image, where the change in cerebral blood flow is indicated by a color scale. The orange area indicates a region with increased blood flow in the brain. The increased brain activity came from mechanically stimulating the whisker of the rat. This technique has been used to map out the 3-D vasculature of the rat brain [96], and can also generate the spectral content at any position as shown in [45]. The technique is sensitive enough to detect the change in blood flow from activity in the brain, which was demonstrated by following an epileptic seizure in a rat brain [62]. The slow moving brain waves could also be detected by following the change in blood flow. The fast plane wave imaging gives an excellent time resolution in the sub-millisecond range combined with sub-millimeter resolution. This unique imaging modality can, thus, follow events with both a high spatial and temporal resolution, which is currently not possible with any other modality.

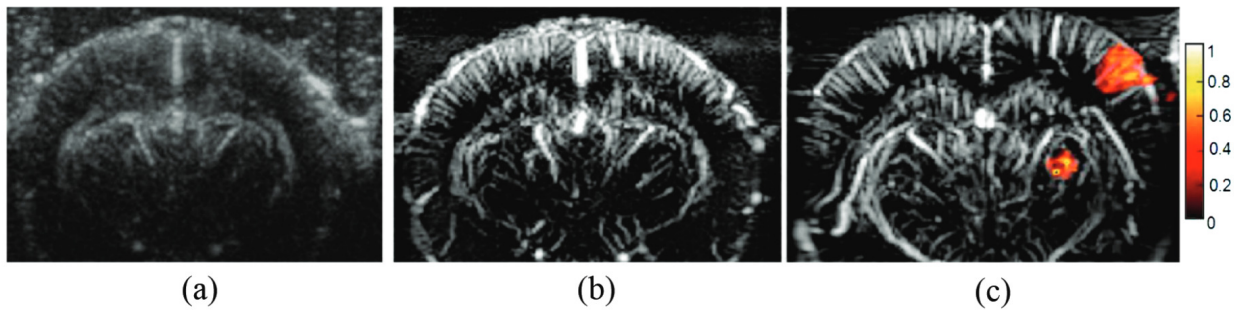


Fig. 9. Cerebral blood flow in a rat using conventional velocity imaging (left) and plane waves (middle image). The right image shows functional ultrasound imaging, where the color indicates change in blood flow due to stimulation of the rats whiskers (from [48]).

VII. DISCUSSION

With the advent of high-frame-rate ultrasound imaging, one may expect an increased clinical interest, since time-resolved high-quality vector flow maps can now be obtained. Parallel acquisition systems in medical ultrasound have shown to give considerable advantages in terms of frame rate, estimation precision and accuracy, and sensitivity for both spherical and plane wave emissions. Several methods for ultra-fast imaging with thousand of frame per second have been developed, which can reveal the true 2-D velocity vector and can quantitatively show complex pulsating flow with turbulence and vortices. The time resolution is in ms, and sub-millimeter resolution has been attained to reveal the true hemodynamics. Early indications also show that these methods can be translated to full 3-D flow with acquisitions of volume data and estimation of the complete 3-D vector.

The major advantage of these systems is the continuously available data for the full image, and the advantages gained from this is really captured in Figs. 7 and 9. Fig. 7 shows the ability to estimate high velocity flow in any direction with a high temporal and spatial resolution. The same type of acquisition sequence is applied in Fig. 9, where low velocity flow is estimated from using many data points and employs averaging. The complete data sets make it possible to decide on the processing after data acquisition, and both the vector velocity, slow flow, and spectral content can be found retrospectively with a high precision.

The resulting data are accurate enough to be used in higher order estimates for e.g. pressure gradient estimation and functional ultrasound imaging. This has led to the development of systems capable of showing brain function with exquisite resolution in both time and space, which are capable of revealing the time course of e.g. epileptic seizures in a rat brain [62].

Several challenges still exist for this type of imaging. The amounts of data and processing demands are huge. Often between 10 GBytes/s of data for 2-D imaging up to to 140 Gbytes/s for fully populated 2-D arrays are acquired per second, which has to be beamformed for full images for every emission. This gives a large data expansion and processing demands are for several Tflops for real time imaging [48]. Currently, no real-time parallel flow systems exist, and there is a real need for faster hardware and more efficient schemes for beamforming. SASB and Fourier beamforming schemes

are attempts to reduce the processing demands by factors of 20 to 64 and can pave the way for real time implementations.

Another challenge is the visualization of flow and how this massive amount of information should be used in the clinic. Especially for 3-D vector flow image and high frame rate methods, it is unclear how to handle this. The introduction of ever faster GPUs with larger bandwidths will in combination with more efficient algorithms ultimately solve the real-time problem and give a large range of interesting flow systems with the capability of deriving useful clinical indices.

ACKNOWLEDGEMENT

This work was supported by grant 82-2012-4 from the Danish National Advanced Technology Foundation, by BK Ultrasound, Herlev, Denmark, and by discovery and accelerating grants of the Natural Sciences and Engineering Research Council of Canada (RPGIN-2016-04042, RGPIN-2015-04217 and RGPAS-477914-2015).

DISCLOSURE

The authors have been involved in the development of many of the techniques presented in this review. Jørgen Arendt Jensen holds patents on SA flow imaging and directional VFI. He earns royalty from the selling of TO VFI systems by BK Ultrasound. Svetoslav Nikolov is employed by BK Ultrasound. Alfred C. H. Yu has a provisional patent on vector projectile imaging that forms the basis of Mindrays V-Flow option.

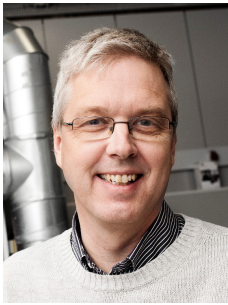
REFERENCES

- [1] J. A. Jensen, S. I. Nikolov, A. Yu, and D. Garcia, "Ultrasound vector flow imaging I: Sequential systems," *IEEE Trans. Ultrason., Ferroelec., Freq. Contr.*, p. Accepted, 2016.
- [2] D. H. Evans and W. N. McDicken, *Doppler Ultrasound, Physics, Instrumentation, and Signal Processing*. New York: John Wiley & Sons, 2000.
- [3] J. A. Jensen, *Estimation of Blood Velocities Using Ultrasound: A Signal Processing Approach*. New York: Cambridge University Press, 1996.
- [4] S. I. Nikolov and J. A. Jensen, "Velocity estimation using synthetic aperture imaging," in *Proc. IEEE Ultrason. Symp.*, 2001, pp. 1409–1412.
- [5] S. I. Nikolov, "Synthetic Aperture Tissue and Flow Ultrasound Imaging," Ph.D. dissertation, Ørsted•DTU, Technical University of Denmark, 2800, Lyngby, Denmark, 2001.
- [6] J. A. Jensen, S. Nikolov, K. L. Gammelmark, and M. H. Pedersen, "Synthetic aperture ultrasound imaging," *Ultrasonics*, vol. 44, pp. e5–e15, 2006.
- [7] J. J. Flaherty, K. R. Erikson, and V. M. Lund, "Synthetic aperture ultrasound imaging systems," United States Patent, US 3,548,642, 1967, united States Patent, US 3,548,642, 1967, Published 22 Dec 1970.

- [8] C. B. Burckhardt, P.-A. Grandchamp, and H. Hoffmann, "An experimental 2 MHz synthetic aperture sonar system intended for medical use," *IEEE Trans. Son. Ultrason.*, vol. 21, no. 1, pp. 1–6, January 1974.
- [9] J. T. Ylitalo and H. Ermert, "Ultrasound synthetic aperture imaging: Monostatic approach," *IEEE Trans. Ultrason., Ferroelec., Freq. Contr.*, vol. 41, pp. 333–339, 1994.
- [10] P. D. Corl, P. M. Grant, and G. S. Kino, "A digital synthetic focus acoustic imaging system for nde," in *Proc. IEEE Ultrason. Symp.*, 1978, pp. 263–268.
- [11] G. S. Kino, D. Corl, S. Bennett, and K. Peterson, "Real time synthetic aperture imaging system," in *Proc. IEEE Ultrason. Symp.*, 1980, pp. 722–731.
- [12] D. K. Peterson and G. S. Kino, "Real-time digital image reconstruction: A description of imaging hardware and an analysis of quantization errors," *IEEE Trans. Son. Ultrason.*, vol. 31, no. 4, pp. 337–351, Jul 1984.
- [13] K. Nagai, "A new synthetic-aperture focusing method for ultrasonic B-scan imaging by the fourier transform," *IEEE Trans. Son. Ultrason.*, vol. SU-32, no. 4, pp. 531–536, 1985.
- [14] M. O'Donnell and L. J. Thomas, "Efficient synthetic aperture imaging from a circular aperture with possible application to catheter-based imaging," *IEEE Trans. Ultrason., Ferroelec., Freq. Contr.*, vol. 39, pp. 366–380, 1992.
- [15] M. Karaman, P. C. Li, and M. O'Donnell, "Synthetic aperture imaging for small scale systems," *IEEE Trans. Ultrason., Ferroelec., Freq. Contr.*, vol. 42, pp. 429–442, 1995.
- [16] M. Karaman and M. O'Donnell, "Subaperture processing for ultrasonic imaging," *IEEE Trans. Ultrason., Ferroelec., Freq. Contr.*, vol. 45, pp. 126–135, 1998.
- [17] G. R. Lockwood and F. Foster, "Design of sparse array imaging systems," in *Proc. IEEE Ultrason. Symp.*, 1995, pp. 1237–1243.
- [18] G. R. Lockwood, J. R. Talman, and S. S. Brunke, "Real-time 3-D ultrasound imaging using sparse synthetic aperture beamforming," *IEEE Trans. Ultrason., Ferroelec., Freq. Contr.*, vol. 45, pp. 980–988, 1998.
- [19] S. I. Nikolov, K. Gammelmark, and J. A. Jensen, "Recursive ultrasound imaging," in *Proc. IEEE Ultrason. Symp.*, vol. 2, 1999, pp. 1621–1625.
- [20] Y. Takeuchi, "An investigation of a spread energy method for medical ultrasound systems - part one: theory and investigations," *Ultrasonics*, pp. 175–182, 1979.
- [21] M. O'Donnell, "Coded excitation system for improving the penetration of real-time phased-array imaging systems," *IEEE Trans. Ultrason., Ferroelec., Freq. Contr.*, vol. 39, pp. 341–351, 1992.
- [22] T. Misaridis and J. A. Jensen, "Use of modulated excitation signals in ultrasound, Part I: Basic concepts and expected benefits," *IEEE Trans. Ultrason., Ferroelec., Freq. Contr.*, vol. 52, pp. 192–207, 2005.
- [23] —, "Use of modulated excitation signals in ultrasound, Part II: Design and performance for medical imaging applications," *IEEE Trans. Ultrason., Ferroelec., Freq. Contr.*, vol. 52, pp. 208–219, 2005.
- [24] —, "Use of modulated excitation signals in ultrasound, Part III: High frame rate imaging," *IEEE Trans. Ultrason., Ferroelec., Freq. Contr.*, vol. 52, pp. 220–230, 2005.
- [25] K. L. Gammelmark and J. A. Jensen, "Multielement synthetic transmit aperture imaging using temporal encoding," *IEEE Trans. Med. Imag.*, vol. 22, no. 4, pp. 552–563, 2003.
- [26] M. H. Pedersen, K. L. Gammelmark, and J. A. Jensen, "In-vivo evaluation of convex array synthetic aperture imaging," *Ultrasound Med. Biol.*, vol. 33, pp. 37–47, 2007.
- [27] W. H. Kim, J. M. Chang, C. Kim, J. Park, Y. Yoo, W. K. Moon, N. Cho, and B. Choi, "Synthetic aperture imaging in breast ultrasound: a preliminary clinical study," *Academic Radiology*, vol. 19, pp. 923–929, 2012.
- [28] R. Y. Chiao, L. J. Thomas, and S. D. Silverstein, "Sparse array imaging with spatially-encoded transmits," in *Proc. IEEE Ultrason. Symp.*, 1997, pp. 1679–1682.
- [29] R. Y. Chiao and L. J. Thomas, "Synthetic transmit aperture using orthogonal golay coded excitation," in *Proc. IEEE Ultrason. Symp.*, 2000, pp. 1469–1472.
- [30] F. Gran and J. A. Jensen, "Frequency division transmission and synthetic aperture reconstruction," *IEEE Trans. Ultrason., Ferroelec., Freq. Contr.*, vol. 53(5), pp. 900–911, 2006.
- [31] —, "Directional velocity estimation using a spatio-temporal encoding technique based on frequency division for synthetic transmit aperture ultrasound," *IEEE Trans. Ultrason., Ferroelec., Freq. Contr.*, vol. 53(7), pp. 1289–1299, 2006.
- [32] —, "Spatial encoding using a code division technique for fast ultrasound imaging," *IEEE Trans. Ultrason., Ferroelec., Freq. Contr.*, vol. 55, no. 1, pp. 12–23, 2008.
- [33] S. I. Nikolov and J. A. Jensen, "In-vivo Synthetic Aperture Flow Imaging in Medical Ultrasound," *IEEE Trans. Ultrason., Ferroelec., Freq. Contr.*, vol. 50, no. 7, pp. 848–856, 2003.
- [34] J. A. Jensen and S. I. Nikolov, "Directional synthetic aperture flow imaging," *IEEE Trans. Ultrason., Ferroelec., Freq. Contr.*, vol. 51, pp. 1107–1118, 2004.
- [35] J. A. Jensen and N. Oddershede, "Estimation of velocity vectors in synthetic aperture ultrasound imaging," *IEEE Trans. Med. Imag.*, vol. 25, pp. 1637–1644, 2006.
- [36] C. A. Villagomez-Hoyos, M. B. Stuart, K. L. Hansen, M. B. Nielsen, and J. A. Jensen, "Accurate angle estimator for high frame rate 2-D vector flow imaging," *IEEE Trans. Ultrason., Ferroelec., Freq. Contr.*, p. Accepted, 2016.
- [37] N. Oddershede and J. A. Jensen, "Effects influencing focusing in synthetic aperture vector flow imaging," *IEEE Trans. Ultrason., Ferroelec., Freq. Contr.*, vol. 54, no. 9, pp. 1811–1825, 2007.
- [38] K. L. Gammelmark and J. A. Jensen, "2-D tissue motion compensation of synthetic transmit aperture images," *IEEE Trans. Ultrason., Ferroelec., Freq. Contr.*, pp. 594–610, April 2014.
- [39] H. Takahashi, H. Hasegawa, and H. Kanai, "Echo speckle imaging of blood particles with high-frame-rate echocardiography," *Japanese Journal of Applied Physics*, vol. 53, no. 07KF08, pp. 1–7, Jul 2014.
- [40] S. Bjærum, H. Torp, and K. Kristoffersen, "Clutter filters adapted to tissue motion in ultrasound color flow imaging," *IEEE Trans. Ultrason., Ferroelec., Freq. Contr.*, vol. 49, no. 6, pp. 693–704, June 2002.
- [41] H. Torp, "Clutter Rejection Filters in Color Flow Imaging: A Theoretical Approach," *IEEE Trans. Ultrason., Ferroelec., Freq. Contr.*, vol. 44, no. 2, pp. 417–424, 1997.
- [42] A. C. H. Yu and L. Løvstakken, "Eigen-based clutter filter design for ultrasound color flow imaging: a review," *IEEE Trans. Ultrason., Ferroelec., Freq. Contr.*, vol. 57, no. 5, pp. 1096–1111, 2010.
- [43] C. Demene, T. Deffieux, M. Perno, B.-F. Osmanski, V. Biran, J.-L. Gennisson, L.-A. Sieu, A. Bergel, S. Franqui, J.-M. Correias, and et al., "Spatiotemporal clutter filtering of ultrafast ultrasound data highly increases doppler and fultrasound sensitivity," *IEEE Trans. Med. Imag.*, vol. 34, no. 11, pp. 2271–2285, 2015.
- [44] K. L. Hansen, J. Udesen, N. Oddershede, L. Henze, C. Thomsen, J. A. Jensen, and M. B. Nielsen, "In vivo comparison of three ultrasound vector velocity techniques to MR phase contrast angiography," *Ultrasonics*, vol. 49, pp. 659–667, 2009.
- [45] J. Bercoff, G. Montaldo, T. Loupas, D. Savary, F. Meziere, M. Fink, and M. Tanter, "Ultrafast compound Doppler imaging: providing full blood flow characterization," *IEEE Trans. Ultrason., Ferroelec., Freq. Contr.*, vol. 58, no. 1, pp. 134–147, January 2011.
- [46] C. A. Villagomez-Hoyos, M. B. Stuart, and J. A. Jensen, "Increasing the dynamic range of synthetic aperture vector flow imaging," in *Proc. SPIE Med. Imag.*, vol. 9040, 2014, pp. 1–12.
- [47] —, "In-vivo high dynamic range vector flow imaging," *Proc. IEEE Ultrason. Symp.*, pp. 1–4, 2015.
- [48] M. Tanter and M. Fink, "Ultrafast imaging in biomedical ultrasound," *IEEE Trans. Ultrason., Ferroelec., Freq. Contr.*, vol. 61, no. 1, pp. 102–119, January 2014.
- [49] H. K. H. So, J. Chen, B. Y. S. Yiu, and A. C. H. Yu, "Medical ultrasound imaging: to GPU or not to GPU?" *IEEE Micro*, vol. 31, no. 5, pp. 54–65, 2011.
- [50] J. Kortbek, J. A. Jensen, and K. L. Gammelmark, "Sequential beamforming for synthetic aperture imaging," *Ultrasonics*, vol. 53, no. 1, pp. 1–16, 2013.
- [51] M. C. Hemmsen, P. M. Hansen, T. Lange, J. M. Hansen, K. L. Hansen, M. B. Nielsen, and J. A. Jensen, "In vivo evaluation of synthetic aperture sequential beamforming," *Ultrasound Med. Biol.*, vol. 38, no. 4, pp. 708–716, 2012.
- [52] A. H. Brandt, M. C. Hemmsen, P. M. Hansen, S. S. Madsen, P. S. Krohn, T. Lange, K. L. Hansen, J. A. Jensen, and M. B. Nielsen, "Clinical evaluation of synthetic aperture harmonic imaging for scanning focal malignant liver lesions," *Ultrasound in Medicine & Biology*, vol. 41, no. 9, pp. 2368–75, 2015.
- [53] Y. Li and J. A. Jensen, "Directional synthetic aperture flow imaging using a dual stage beamformer approach," in *Proc. IEEE Ultrason. Symp.*, 2011, pp. 1254–1257.
- [54] M. C. Hemmsen, L. Lassen, T. Kjeldsen, J. Mosegaard, and J. A. Jensen, "Implementation of real-time duplex synthetic aperture ultrasonography," in *Proc. IEEE Ultrason. Symp.*, 2015, pp. 1–4.
- [55] M. Tanter, J. Bercoff, L. Sandrin, and M. Fink, "Ultrafast compound imaging for 2-D motion vector estimation: application to transient elastography," *IEEE Trans. Ultrason., Ferroelec., Freq. Contr.*, vol. 49, pp. 1363–1374, 2002.

- [56] J. Bercoff, M. Tanter, L. Sandrin, S. Catheline, and M. Fink, "Ultrafast compound imaging for 2-d displacement vector measurements: application to transient elastography and color flow mapping," in *Proc. IEEE Ultrason. Symp.*, 2001, pp. 1619–1622.
- [57] L. Sandrin, S. Manneville, and M. Fink, "Ultrafast two-dimensional ultrasonic speckle velocimetry: A tool in flow imaging," *Appl. Phys. Lett.*, vol. 78, no. 8, pp. 1155–1157, 2001.
- [58] J. Udesen, F. Gran, and J. A. Jensen, "Fast Color Flow Mode Imaging Using Plane Wave Excitation and Temporal Encoding," in *Proc. SPIE - Progress in biomedical optics and imaging*, vol. 5750, Feb. 2005, pp. 427–436.
- [59] J. Udesen, F. Gran, K. L. Hansen, J. A. Jensen, C. Thomsen, and M. B. Nielsen, "High frame-rate blood vector velocity imaging using plane waves: simulations and preliminary experiments," *IEEE Trans. Ultrason., Ferroelec., Freq. Contr.*, vol. 55, no. 8, pp. 1729–1743, 2008.
- [60] S. Fadnes, S. A. Nyrnes, H. Torp, and L. Løvstakken, "Shunt flow evaluation in congenital heart disease based on two-dimensional speckle tracking," *Ultrasound Med. Biol.*, vol. 40, no. 10, pp. 2379–2391, 2014.
- [61] S. K. Jespersen, J. E. Wilhjelm, and H. Sillesen, "Multi-angle compound imaging," *Ultrason. Imaging*, vol. 20, pp. 81–102, 1998.
- [62] E. Mace, G. Montaldo, I. Cohen, M. Baulac, M. Fink, and M. Tanter, "Functional ultrasound imaging of the brain," *Nature methods*, vol. 8, no. 8, pp. 662–664, 2011.
- [63] E. Mace, G. Montaldo, B. Osmanski, I. Cohen, M. Fink, and M. Tanter, "Functional ultrasound imaging of the brain: theory and basic principles," *IEEE Trans. Ultrason., Ferroelec., Freq. Contr.*, vol. 60, no. 3, pp. 492–506, 2013.
- [64] J. A. Jensen, O. Holm, L. J. Jensen, H. Bendsen, S. I. Nikolov, B. G. Tomov, P. Munk, M. Hansen, K. Salomonsen, J. Hansen, K. Gormsen, H. M. Pedersen, and K. L. Gammelmark, "Ultrasound research scanner for real-time synthetic aperture image acquisition," *IEEE Trans. Ultrason., Ferroelec., Freq. Contr.*, vol. 52 (5), pp. 881–891, May 2005.
- [65] P. Tortoli, L. Bassi, E. Boni, A. Dallai, F. Guidi, and S. Ricci, "ULA-OP: An advanced open platform for ultrasound research," *IEEE Trans. Ultrason., Ferroelec., Freq. Contr.*, vol. 56, no. 10, pp. 2207–2216, Oct. 2009.
- [66] R. E. Daigle and P. J. Kaczowski, "High frame rate quantitative Doppler flow imaging using unfocused transmit beams," 2009, uS Patent Application 12/490,780.
- [67] J. A. Jensen, H. Holtén-Lund, R. T. Nilsson, M. Hansen, U. D. Larsen, R. P. Domsten, B. G. Tomov, M. B. Stuart, S. I. Nikolov, M. J. Pihl, Y. Du, J. H. Rasmussen, and M. F. Rasmussen, "SARUS: A synthetic aperture real-time ultrasound system," *IEEE Trans. Ultrason., Ferroelec., Freq. Contr.*, vol. 60, no. 9, pp. 1838–1852, 2013.
- [68] C. C. P. Cheung, A. C. H. Yu, N. Salimi, B. Y. S. Yiu, I. K. H. Tsang, B. Kerby, R. Z. Azar, and K. Dickie, "Multi-channel pre-beamformed data acquisition system for research on advanced ultrasound imaging methods," *IEEE Trans. Ultrason., Ferroelec., Freq. Contr.*, vol. 59, no. 2, pp. 243–253, 2012.
- [69] M. Walczak, M. Lewandowski, and N. Zolek, "Optimization of real-time ultrasound PCIe data streaming and OpenCL processing for SAFT imaging," in *Proc. IEEE Ultrason. Symp.*, 2013, pp. 2064–2067.
- [70] —, "A real-time streaming DAQ for Ultrasonix research scanner," in *Proc. IEEE Ultrason. Symp.*, 2014, pp. 1257–1260.
- [71] S. Ricci, L. Bassi, and P. Tortoli, "Real-time vector velocity assessment through multigate Doppler and plane waves," *IEEE Trans. Ultrason., Ferroelec., Freq. Contr.*, vol. 61, no. 2, pp. 314–324, 2014.
- [72] S. Ricci, D. Vilkomerson, R. Matera, and P. Tortoli, "Accurate blood peak velocity estimation using spectral models and vector Doppler," *IEEE Trans. Ultrason., Ferroelec., Freq. Contr.*, vol. 62, no. 4, pp. 686–696, 2015.
- [73] B. Y. Yiu, S. S. Lai, and A. C. Yu, "Vector projectile imaging: time-resolved dynamic visualization of complex flow patterns," *Ultrasound Med. Biol.*, vol. 40, no. 9, pp. 2295–2309, sept 2014.
- [74] I. K. Ekroll, A. Swillens, P. Segers, T. Dahl, H. Torp, and L. Løvstakken, "Simultaneous quantification of flow and tissue velocities based on multi-angle plane wave imaging," *IEEE Trans. Ultrason., Ferroelec., Freq. Contr.*, vol. 60, no. 4, pp. 727–738, 2013.
- [75] S. Fadnes, I. K. Ekroll, S. A. Nyrnes, H. Torp, and L. Løvstakken, "Robust angle-independent blood velocity estimation based on dual-angle plane wave imaging," *IEEE Trans. Ultrason., Ferroelec., Freq. Contr.*, vol. 62, no. 10, pp. 1757–1767, October 2015.
- [76] J. Flynn, R. Daigle, L. Pflugrath, P. Kaczowski, and K. Linkhart, "Estimation and display for vector Doppler imaging using planewave transmissions," *Proc. IEEE Ultrason. Symp.*, pp. 413–418, 2011.
- [77] J. Flynn, R. Daigle, L. Pflugrath, and P. Kaczowski, "High frame rate vector velocity blood flow imaging using a single plane wave transmission angle," in *Proc. IEEE Ultrason. Symp.*, 2012, pp. 323–325.
- [78] A. C. H. Yu and Y. S. Yiu, "Apparatus for ultrasound flow vector imaging and methods thereof," 2014, patent Application PCT/CN2014/091035.
- [79] F. Gran, J. Udesen, M. B. Nielsen, and J. A. Jensen, "Coded ultrasound for blood flow estimation using subband processing," *IEEE Trans. Ultrason., Ferroelec., Freq. Contr.*, vol. 55, no. 10, pp. 2211–2220, 2008.
- [80] S. Salles, A. J. Y. Chee, D. Garcia, A. C. H. Yu, D. Vray, and H. Liebgott, "2-D arterial wall motion imaging using ultrafast ultrasound and transverse oscillations," *IEEE Trans. Ultrason., Ferroelec., Freq. Contr.*, vol. 62, no. 6, pp. 1047–1058, 2015.
- [81] M. Lenge, A. Ramalli, P. Tortoli, C. Cachard, and H. Liebgott, "Plane-wave transverse oscillation for high-frame-rate 2-D vector flow imaging," *IEEE Trans. Ultrason., Ferroelec., Freq. Contr.*, vol. 62, no. 12, pp. 2126–2137, December 2015.
- [82] D. P. Shattuck, M. D. Weinshenker, S. W. Smith, and O. T. von Ramm, "Explosocan: A parallel processing technique for high speed ultrasound imaging with linear phased arrays," *J. Acoust. Soc. Am.*, vol. 75, pp. 1273–1282, 1984.
- [83] T. Misaridis and J. A. Jensen, "Space-time encoding for high frame rate ultrasound imaging," *Ultrasonics*, vol. 40, pp. 593–597, 2002.
- [84] L. Tong, A. Ramalli, R. Jasaityte, P. Tortoli, and J. D'Hooge, "Multi-transmit beam forming for fast cardiac imaging - experimental validation and in vivo application," *IEEE Trans. Med. Imag.*, vol. 33, no. 6, pp. 1205–1219, 2014.
- [85] N. Oddershede, F. Gran, and J. A. Jensen, "Multi-frequency encoding for fast color flow or quadroplex imaging," *IEEE Trans. Ultrason., Ferroelec., Freq. Contr.*, vol. 55, no. 4, pp. 778–786, April 2008.
- [86] S. Holbek, M. J. Pihl, C. Ewertsen, M. B. Nielsen, and J. A. Jensen, "In vivo 3-D vector velocity estimation with continuous data," in *Proc. IEEE Ultrason. Symp.*, 2015, pp. 1–4.
- [87] S. Holbek, T. L. Christiansen, M. Stuart, C. Beers, E. V. Thomsen, and J. A. Jensen, "3-D vector flow estimation with row-column addressed arrays," *IEEE Trans. Ultrason., Ferroelec., Freq. Contr.*, 2016.
- [88] J. A. Jensen and S. I. Nikolov, "A method for real-time three-dimensional vector velocity imaging," in *Proc. IEEE Ultrason. Symp.*, 2003, pp. 1582–1585.
- [89] J. Provost, C. Papadacci, J. E. Arango, M. Imbault, M. Fink, J. L. Gennisson, M. Tanter, and M. Pernot, "3-D ultrafast ultrasound imaging in vivo," *Phys. Med. Biol.*, vol. 59, no. 19, pp. L1–L13, 2014.
- [90] K. L. Hansen, J. Udesen, F. Gran, J. A. Jensen, and M. B. Nielsen, "In-vivo examples of flow patterns with the fast vector velocity ultrasound method," *Ultraschall in Med.*, vol. 30, pp. 471–476, 2009.
- [91] —, "Fast blood vector velocity imaging using ultrasound, in-vivo examples of complex blood flow in the vascular system," in *Proc. IEEE Ultrason. Symp.*, 2008, pp. 1068–1071.
- [92] H. Abe, G. Caracciolo, A. Kheradvar, G. Pedrizzetti, B. K. Khandheria, J. Narula, and P. P. Sengupta, "Contrast echocardiography for assessing left ventricular vortex strength in heart failure: a prospective cohort study," *European Heart Journal - Cardiovascular Imaging*, vol. 14, no. 11, pp. 1049–1060, Nov 2013.
- [93] M. Cikes, L. Tong, G. R. Sutherland, and J. D'hooge, "Ultrafast cardiac ultrasound imaging: technical principles, applications, and clinical benefits," *JACC. Cardiovascular imaging*, vol. 7, no. 8, pp. 812–823, 2014.
- [94] C. Moore, J. Castellucci, M. Andersen, M. Lefevre, K. Arges, J. Kisslo, and O. von Ramm, "Live high-frame-rate echocardiography," *IEEE Trans. Ultrason., Ferroelec., Freq. Contr.*, vol. 62, no. 10, pp. 1779–1787, Oct 2015.
- [95] P. Angelelli, S. R. Snare, S. A. Nyrnes, S. Bruckner, H. Hauser, and L. Løvstakken, "Live ultrasound-based particle visualization of blood flow in the heart," in *Proceedings of the 30th Spring Conference on Computer Graphics*, 2014, pp. 42–49.
- [96] C. Demene, E. Tiran, L.-A. Sieu, A. Bergel, J. L. Gennisson, M. Pernot, T. Deffieux, I. Cohen, and M. Tanter, "4d microvascular imaging based on ultrafast doppler tomography," *Neuroimage*, 2015.

BIBLIOGRAPHIES



Jørgen Arendt Jensen earned his Master of Science in electrical engineering in 1985 and the PhD degree in 1989, both from the Technical University of Denmark. He received the Dr.Techn. degree from the university in 1996. He has since 1993 been full professor of Biomedical Signal Processing at the Technical University of Denmark at the Department of Electrical Engineering and head of Center for Fast Ultrasound Imaging since its inauguration in 1998. He has published more than 450 journal and conference papers on signal processing and medical ultrasound and the book "Estimation of Blood Velocities Using Ultrasound", Cambridge University Press in 1996. He is also the developer and maintainer of the Field II simulation program. He has been a visiting scientist at Duke University, Stanford University, and the University of Illinois at Urbana-Champaign. He was head of the Biomedical Engineering group from 2007 to 2010. In 2003 he was one of the founders of the biomedical engineering program in Medicine and Technology, which is a joint degree program between the Technical University of Denmark and the Faculty of Health and Medical Sciences at the University of Copenhagen. The degree is one of the most sought after engineering degrees in Denmark. He was chairman of the study board from 2003-2010 and adjunct professor at the University of Copenhagen from 2005-2010. He has given a number of short courses on simulation, synthetic aperture imaging, and flow estimation at international scientific conferences and teaches biomedical signal processing and medical imaging at the Technical University of Denmark. He has given more than 60 invited talks at international meetings, received several awards for his research, and is an IEEE Fellow. His research is centered around simulation of ultrasound imaging, synthetic aperture imaging, vector blood flow estimation, and construction of ultrasound research systems.



Svetoslav Ivanov Nikolov got his Master of Science in electrical engineering in 1996 from the Technical University - Sofia (TU - Sofia), and a Ph.D. degree in 2001 from the Technical University of Denmark

(DTU). From 2001 till 2009 he was an Associate Professor in Electronics and Signal Processing at DTU. Svetoslav Nikolov is Senior IEEE Member since 2011 for his pioneering work in the field of synthetic aperture imaging and flow estimation. In 2008, he joined BK Medical Aps to work on the commercial implementation of the technologies developed at DTU. He is an Analogic Fellow since 2015 as a recognition for his work in research and development.



Alfred C. H. Yu (S99-M07-SM12) is an Associate Professor in the Department of Electrical and Computer Engineering at the University of Waterloo, ON, Canada. He has a long-standing research interest in ultrasound imaging innovations and therapeutic ultrasound discoveries. Alfred obtained his undergraduate degree in Electrical Engineering from the University of Calgary in 2002, and he received his M.A.Sc. and Ph.D. degrees in Biomedical Engineering from the University of Toronto in 2004 and 2007. He also interned at Philips Research North America in 2005. Before he relocated to Waterloo, Alfred was a Research Assistant Professor at the University of Hong Kong, where he founded and served as the Principal Investigator of HKU Biomedical Ultrasound Laboratory. Alfred is a Senior Member of IEEE and AIUM. He is an Associate Editor of *IEEE Transactions on Ultrasonics, Ferroelectrics, and Frequency Control* and an Editorial Board Member of *Ultrasound in Medicine and Biology*. He also serves on the Technical Program Committee of *IEEE Ultrasonics Symposium* and *International Symposium for Therapeutic Ultrasound*.



Damien Garcia obtained his engineer degree in Mechanical Engineering from the cole Centrale de Marseille, France, in 1997, and received his Ph.D. degree in Biomedical Engineering from the University of Montreal, Canada, in 2003. He was a postdoctoral fellow from 2006 to 2008 in the Department of Echocardiography,

Gregorio Marañón hospital, Madrid, Spain. He is director of the Research Unit of Biomechanics & Imaging in Cardiology (RUBIC) at the University of Montreal Hospital Research Centre (CRCHUM), and assistant professor at the Department of Radiology, Radio-Oncology and Nuclear Medicine at the University of Montreal. He is an Associate Editor of *IEEE Transactions on Ultrasonics, Ferroelectrics, and Frequency Control* and is on the Technical Program Committee of the *IEEE Ultrasonics Symposium*. His clinical and fundamental research interests are in cardiac/cardiovascular ultrasound imaging, mostly in fluid dynamics and flow imaging. A detailed list of his publications is available at www.biomecardio.com